BIOCHEMICAL PHARMACOLOGY 76 (2008) 831–840

available at www.sciencedirect.com

ScienceDirect

journal homepage: www.elsevier.com/locate/biochempharm

Virus entry inhibition by chlorite-oxidized oxyamylose versus induction of antiviral interferon by poly(I:C)

Sandra Li, Erik Martens, Chris Dillen, Philippe E. Van den Steen, Ghislain Opdenakker *

Laboratory of Immunobiology, Rega Institute for Medical Research, University of Leuven, Leuven, Belgium

ARTICLE INFO

Article history:
Received 21 May 2008
Accepted 17 July 2008

Keywords:
COAM
Polyanion
Polysaccharide
Antiviral
Entry inhibition
Interferon

ABSTRACT

Unlike polyribonucleotides, such as poly(I:C), chlorite-oxidized oxyamylose (COAM) has been poorly characterized as a polyanionic antiviral. COAM possesses a controversial interferon (IFN)-inducing capacity and its mechanism of action has not been elucidated. In this study, COAM was biochemically characterized and fractionated according to molecular mass. In comparison with a strong IFN induction and upregulation of the helicase RIG-I and MDA-5 mRNAs by poly(I:C), COAM did not enhance IFN-α or -β and IFN-inducible RNA helicases in mouse fibroblastoid cells. Instead, COAM inhibited virus entry by blocking the attachment to the cells. These results suggest that COAM can alter the outcome of infection, not by IFN induction and in turn modifying the cellular antiviral state, but through inhibition of virus entry into cells.

1. Introduction

The use of monosaccharide derivatives, in particular glucose-derived iminosugars, with antiviral activity against a broad spectrum of viruses is well established. Iminosugar derivatives inhibit viral protein folding and secretion and reduce the infectivity of newly released viral particles, as described for *Human immunodeficiency virus* [1], *Hepatitis B virus* [2], *Bovine viral diarrhea virus* [3,4], *Dengue virus*, *Japanese encephalitis virus* and *West Nile virus* [5]. In comparison to monosaccharide derivatives, little is known about the exact mechanism of antiviral action of certain polysaccharide derivatives, specifically the chlorite-oxidized oxypolysaccharides, which are synthetic polyanions with a polyacetal backbone [6]. Within this group of polyacetal carboxylic acids, chlorite-oxidized oxyamylose (COAM) is the major representative, containing antiviral potencies against viruses of different families including *Influenza virus* [7], *Foot-and-mouth disease virus* [8], *Vaccinia virus*, *Vesicular stomatitis virus* and *Semliki Forest virus* [9] and herpes simplex virus 1 [10]. The mode of action of COAM is controversial. COAM is thought to protect mice from systemic viral infection through the enhancement of interferon (IFN) production, according to the appearance of small amounts of IFN in the serum of mice upon treatment with high doses of COAM [9]. Other large polyanionic molecules, such as the polysaccharides dextran sulfate and heparin have antiviral effects specifically against several enveloped viruses [11] by inhibiting virus entry into cells through association either with viral or cellular receptors [12,13]. Based on its polyanionic nature and in line with the suggested IFN induction, COAM might bear a resemblance to the polyanion polyriboinosinic–polyribocytidylic acid (poly(I:C)). This synthetic double-stranded (ds) RNA analogue mimics viral infection as dsRNA operates as a molecular pattern associated with viral infection, and is generated by many viruses as an intermediate at some point during their replication cycle [14]. dsRNA is

* *Corresponding author at*: Laboratory of Immunobiology, Department of Microbiology and Immunology, Rega Institute for Medical Research, University of Leuven, Minderbroedersstraat 10, B 3000 Leuven, Belgium. Tel.: +32 16337341; fax: +32 16337340.
E-mail address: Ghislain.Opdenakker@rega.kuleuven.be (G. Opdenakker).
0006-2952/$ – see front matter
doi:10.1016/j.bcp.2008.07.022

recognized by the innate immune system through several mechanisms, which trigger a prompt antiviral response resulting in the secretion of antiviral type I IFN-α and -β and proinflammatory cytokines. Amongst the pathogen recognition receptors recognizing viral dsRNA as well as poly(I:C), is Toll-like receptor 3 (TLR-3) which, as a membrane-bound sensor, can recognize both extracellular and endosomal phagocytosed dsRNA [15,16]. The TLR-3 pathway is suggested to contribute to innate immune responses against many viruses including *Influenza virus* [17], *Respiratory syncytial virus* [18], herpes simplex virus 2 [19] and murine cytomegalovirus [20]. Cytosolic detection of viral dsRNA and poly(I:C) is mediated through the helicase family members retinoic-acid-inducible gene I (RIG-I) and melanoma-differentiation-associated gene 5 (MDA-5) thus allowing to directly sense intracellular viral infection in a TLR-3 independent way [21–23]. In vitro studies have shown that RIG-I and MDA-5, defined as RIG-I-like receptors (RLRs), are both capable of responding to poly(I:C) and RNA viruses [24]. However, they preferentially recognize different groups of RNA viruses. Studies using RIG-I and MDA-5-deficient mice reveal that RIG-I is essential in responding to paramyxoviruses, flaviviruses, orthomyxoviruses and rhabdoviruses, whereas MDA-5 is critical in eliciting host antiviral responses against picornaviruses [21,25,26]. The TLR-3 and RLR pathways are the two main and distinct routes of dsRNA detection, both instigating IFN transcription through activation of the transcription factors interferon regulatory factor 3 (IRF-3) and nuclear factor-κB [23]. Type I IFN plays a central role in initiating antiviral innate immunity and modulating subsequent adaptive immunity in vertebrate hosts. This cytokine provides an early line of defense against virus infections by instantly causing cells to adopt a strong antiviral state and by exerting several immune-regulatory actions aimed at preventing virus spread, this through the production of proteins with antiviral, antiproliferative and immunomodulatory activities [27,28]. Stimulation of the IFN pathway can result in ameliorating the outcome of a viral infection.

COAM has been described long ago as an antiviral compound in different virus models including mengovirus infection [9]. Mengovirus is a highly virulent murine strain of *Encephalomyocarditis virus* (EMCV) and belongs, together with Theiler's murine encephalomyelitis virus to the genus *Cardiovirus* of the picornavirus family, causing acute myocarditis and encephalitis in mice. In this study, we investigated in detail the in vitro antiviral profile of COAM against mengovirus, studied direct or indirect mechanisms on the mode of action, and established, against the common concept, that it does not induce IFN.

2. Materials and methods

2.1. Virus and cell culture

L929 fibroblastoid cells were cultured in minimal essential medium (MEM; Invitrogen, Paisley, UK), supplemented with 10% heat-inactivated fetal calf serum (FCS; Hyclone, Logan, UT, USA), 2 mM L-glutamin (Invitrogen) and 0.1% sodium bicarbonate (Invitrogen). Mengovirus was propagated as described [9]. The maintenance medium for virus propagation on monolayers of L929 cells contained 2% FCS. Cells and virus were cultured at 37 °C in a 5% CO_2 atmosphere. Mengovirus stock titers were determined by endpoint titration for the calculation of the 50% cell culture infective dose ($CCID_{50}$).

2.2. Compounds

COAM, a polyacetal carboxylic acid, is a polysaccharide-derived polyanion with a backbone consisting of –C–C–O–C–O– sequences with two attached carboxyl groups. COAM was prepared by a two-step oxidation of amylose, as described previously [6]. In the first oxidation step with periodate, cyclic monosaccharide structures were cleaved between two carbon atoms, yielding a polymer containing two aldehyde functions, called oxyamylose. The aldehyde functions are converted into carboxyl functions by oxidation with sodium chlorite. The endotoxin content of the product batches were determined by the Limulus amebocyte lysate test (Lonza, Verviers, Belgium). The COAM preparations were subjected to SDS-PAGE electrophoresis and any protein contamination was visualized with Coomassie Brilliant Blue R-250 (Sigma–Aldrich, St. Louis, MO, USA) or with silver staining (Silverquest™ Silver Staining Kit; Invitrogen). For mass spectrometry analysis, COAM (1 μg) was dissolved in 30 μl of 50% CH_3CN/ 50% H_2O/ 0.1% CH_3COOH and was analyzed by electrospray ion-trap mass spectrometry in the negative mode with an Esquire_LC apparatus (Bruker, Bremen, Germany). Poly(I:C) was obtained from Sigma–Aldrich. All compounds were resuspended in sterile phosphate buffered saline (PBS; Lonza) for experimental use. Other chemicals used in mass spectrometry analysis and chromatography were purchased from Sigma–Aldrich.

2.3. Gel filtration chromatography

COAM preparations were fractionated by molecular sieving. For analytical fractionation, samples of 50 mg COAM from two different syntheses were applied on a Superdex 200 10/300 GL column (GE Healthcare, Chalfont St. Giles, UK) and equilibrated with 0.1 M NH_4HCO_3 pH 7.8 at a flow rate of 0.3 ml/min. Fractions of 0.4 ml were collected and, after lyophilization, the COAM content was quantified by weight. Subsequently, 8 fractions containing in total 7.9 mg high MW COAM were pooled and concentrated for rechromatography under the same conditions. Preparative fractionation of COAM was obtained with 700 mg preparation on a Hiload 16/60 Superdex 200 column (GE Healthcare) in 0.1 M NH_4HCO_3 pH 7.8 at a flow rate of 0.5 ml/min. Fractions of 0.4 ml were lyophilized and the COAM content was quantified. The columns were calibrated with a protein mix containing thyroglobulin (669 kDa), ferritin (440 kDa), IgG (150 kDa), bovine serum albumin (67 kDa), ovalbumin (43 kDa), cytochrome c (13 kDa) and vitamin B12 (1355 Da), all purchased from Sigma–Aldrich. The sizes of the COAM variants (and fractions) were expressed in relative protein equivalent molecular weights.

2.4. RNA extraction

Viral RNA from cell culture supernatant and total cellular RNA was extracted using the E.Z.N.A.™ Viral RNA Kit (Omega Bio-Tek, Doraville, GA, USA) and the E.Z.N.A.™ Total RNA Mini Kit

(Omega Bio-Tek), respectively. Extractions were performed according to the manufacturer's instructions.

2.5. Absolute quantitation of mengovirus RNA by qRT-PCR

Using Primer Express v2.0 software (Applied Biosystems, Foster City, CA, USA), optimal primer and probe targets that are compatible with TaqMan® PCR requirements were selected to amplify a region of 67 nucleotides in the mengovirus 3D gene that is encoding the RNA-dependent RNA polymerase. (forward primer: 5′-CCG ACA TTG TCT ATC AGA CAT TCC-3′(Operon Biotechnologies, Cologne, Germany); reverse primer: 5′-TTG GCG GCT TGT ACC TTC TC-3′c (Operon Biotechnologies); TaqMan® probe: 5′-CAA GGA CGA GCT TAG AC-3′ (Applied Biosystems)). The TaqMan® probe was labeled with 6-carboxy-fluorescein (FAM) at the 5′-end and contained a non-fluorescent quencher and a minor groove binder at the 3′-end. Quantitative RT-PCR (qRT-PCR) assays were performed using the Eurogentec One step RT qPCR kit (Eurogentec, Seraing, Belgium) in an ABI Prism 7000 Sequence Detection System (Applied Biosystems) and analyzed with Sequence Detection System software version 2.1 (Applied Biosystems). Reactions were carried out in a final volume of 25 μl containing 5 μl of extracted RNA or standard cRNA, 12.5 μl of One step RT qPCR Mastermix containing ROX as a passive reference, 900 nM forward and reverse primer, 200 nM probe and 0.125 μl Euroscript/RNase Inhibitor. Reverse transcription was initiated at 48 °C for 30 min, followed by PCR activation at 95 °C for 10 min and a two-step amplification program of 45 cycles at 95 °C for 15 s and 60 °C for 1 min. The FAM reporter dye signal was measured against the internal ROX reference dye to normalize for non-PCR-related fluorescence emissions. The threshold cycle (Ct) was defined as the fractional cycle number at which the reporter fluorescence, generated by cleavage of the probe, reaches a threshold defined as 10 times the standard deviation of the mean baseline emission calculated for PCR cycles 3 tot 15. To calculate the absolute number of viral genome copies, a mengovirus cRNA standard was made through in vitro transcription with the MEGAshortscript™ T7 High Yield Transcription Kit (Ambion, Austin, TX, USA) as described previously [29]. Briefly, the TaqMan® mengovirus forward primer was modified with a T7 promotor sequence at its 5′-end (5′-TAA TAC GAC TCA CTA TAG GGA GG). PCR products amplified with the modified primer pair were quantified spectrophotometrically at 260 nm. After in vitro transcription and purification of 200 ng of the PCR products, the OD_{260} was determined and quantitation of cRNA was done in duplicate and converted to the molecule number [30].

2.6. Relative quantitation of IFN, RIG-I and MDA-5 mRNA by qRT-PCR

Primer and probe mixes specific for mouse IFN-α4, IFN-β, RIG-I or MDA-5 were purchased from Applied Biosystems. qRT-PCR reactions were carried out in a total volume of 20 μl, containing 125 ng of extracted RNA, 10 μl of One step RT qPCR Mastermix, 1 μl primer/probe mix and 0.2 μl Euroscript/RNase Inhibitor. The qRT-PCR conditions consisted of an RT step at 48 °C for 30 min, an activation step at 95 °C for 10 min followed by 40 cycles of 15 s at 95 °C and 1 min at 60 °C. 18S rRNA (Applied Biosystems) was included as an endogenous reference gene for normalization of target mRNA transcripts. The fold change in gene expression normalized to 18S rRNA and relative to the untreated control was determined according to the comparative ΔΔCt method [31].

2.7. Antiviral experiments using a cell viability assay or qRT-PCR

L929 cells were seeded in 96-well plates at 10,000 cells per well and incubated for 3 days until confluency was reached. Cells were treated with different concentrations of COAM and inoculated with mengovirus at 10 $CCID_{50}$. Mock-infected controls and untreated virus controls were included. After 48 h incubation at 37 °C, cell viability was scored by the 3-(4,5-dimethyl-thiazol-2-yl)-5-(3-carboxymethoxyphenyl)-2-(4-sulfophenyl)-2H-tetrazolium salt (MTS)-based colorimetric assay (Promega, Leiden, The Netherlands). The number of viable cells per well was quantified after a 3-h incubation with MTS in which the reduction of MTS by mitochondrial dehydrogenases to a soluble colored formazan was measured in a spectrophotometer at 492 nm. The percentage cell viability was calculated [32] in order to determine the antiviral activity and cytotoxicity. Estimation of the reduction of viral replication was conducted in a separate experiment with a similar set-up. Cells were inoculated with virus and treated with COAM during 24 h at 37 °C. Viral extracts of the culture supernatants were subjected to mengovirus qRT-PCR.

2.8. Virucidal assay

Virucidal activity was evaluated by the exposure of mengovirus to different concentrations of COAM. Equal volumes of a mengovirus suspension containing 10 $CCID_{50}$ and COAM were mixed and incubated at 37 °C during 2, 4 or 6 h. After each incubation period, the virus/drug mixtures were diluted 100-fold to achieve final COAM concentrations with no inhibitory effect and plated on L929 monolayers to initiate infection. Residual infectivity was determined by cell viability scoring with the MTS assay.

2.9. Time-of-addition study

The antiviral activity of COAM was evaluated at various time points during mengovirus infection. Confluent monolayers of L929 cells were infected with a mengovirus input of 10 $CCID_{50}$ and subsequently treated with 1 mg/ml COAM during viral infection for 1 h, during viral infection and throughout an incubation period for 12 h, or for different time intervals after infection. Cell culture supernatants were harvested at 12 h p.i. and viral RNA was extracted and subjected to mengovirus qRT-PCR.

2.10. Virus attachment assay

Antiviral activity during the process of viral attachment to L929 cells was assessed. L929 monolayers were seeded in 24-well plates, grown until confluency and were pre-chilled at 4 °C. The monolayers were inoculated with 100 $CCID_{50}$

mengovirus in the absence or presence of COAM concentrations ranging from 0.1 to 1000 μg/ml, each concentration in triplicate. Virus in the absence or presence of COAM was allowed to attach for 60 min at 4 °C, medium was aspirated and cells were washed three times with PBS to remove any unattached virus particles. The monolayers were then incubated for a further 8 h. After three consecutive freeze/thaw cycles, bound virus particles were measured with mengovirus qRT-PCR. Endocytosis does not occur at a low temperature of 4 °C, thus a one-hour incubation at 4 °C permits the attachment of the virus to the cells, but not endocytosis.

2.11. Induction assays

L929 cells were plated in a 24-well format and incubated until confluency was reached. The cells were treated with 1 mg/ml COAM or 10 μg/ml poly(I:C). Untreated control cells were included. At the indicated time points, culture supernatant was collected, total cellular RNA was isolated and mRNA expression levels for IFN-α4, IFN-β, RIG-I and MDA-5 were determined by qRT-PCR. IFN-α and -β protein concentrations in L929 supernatants were quantified using the VeriKine™ Mouse Interferon Alpha ELISA Kit and Verikine™ Mouse Interferon Beta ELISA Kit (PBL InterferonSource, Piscataway, NJ, USA), respectively, and according to the manufacturer's instructions.

2.12. Statistical analysis

All results are shown as mean ± S.E.M. Statistical analyses were performed using Prism® 5 software (GraphPad, San Diego, CA, USA). Differences between treatment and control groups were evaluated using the Mann–Whitney test. A p-value of <0.05 was considered statistically significant.

3. Results

3.1. Synthesis and purification of COAM

COAM (Fig. 1A) was synthesized as described [6] and the preparations were structurally and biochemically analyzed by electrospray ion-trap mass spectrometry. Because of the size

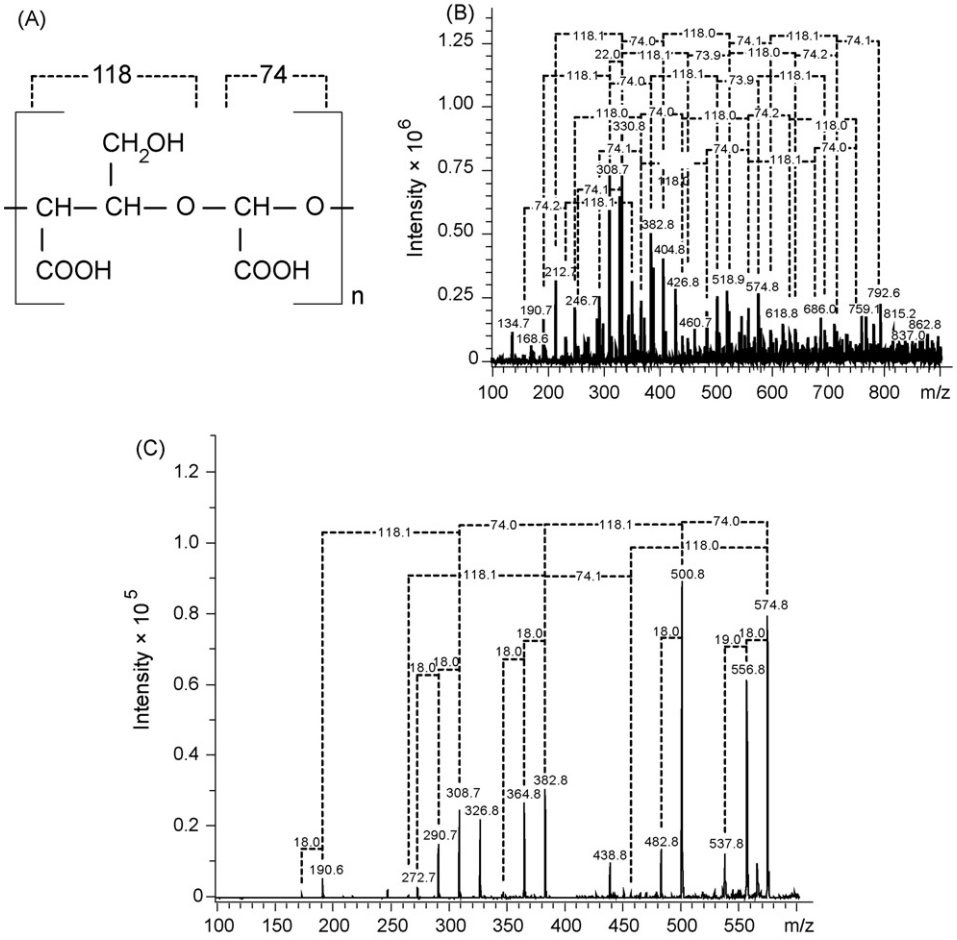

Fig. 1 – Structural analysis of COAM by mass spectrometry. (A) The structural unit of COAM is shown, with alternating subunits, as derived from glucose units in amylose. The calculated mono-isotopic masses of these subunits are also indicated. (B) COAM was subjected to electrospray ion-trap mass spectrometry in the negative mode. Mostly single charged ions were observed. The mono-isotopic masses of particular individual ions are indicated on top of the peaks. Mass differences between ions of specific fragmentation series are also indicated. (C) One ion (574.8 Da), observed in the spectrum of panel B, was isolated in the trap and further fragmented and analyzed.

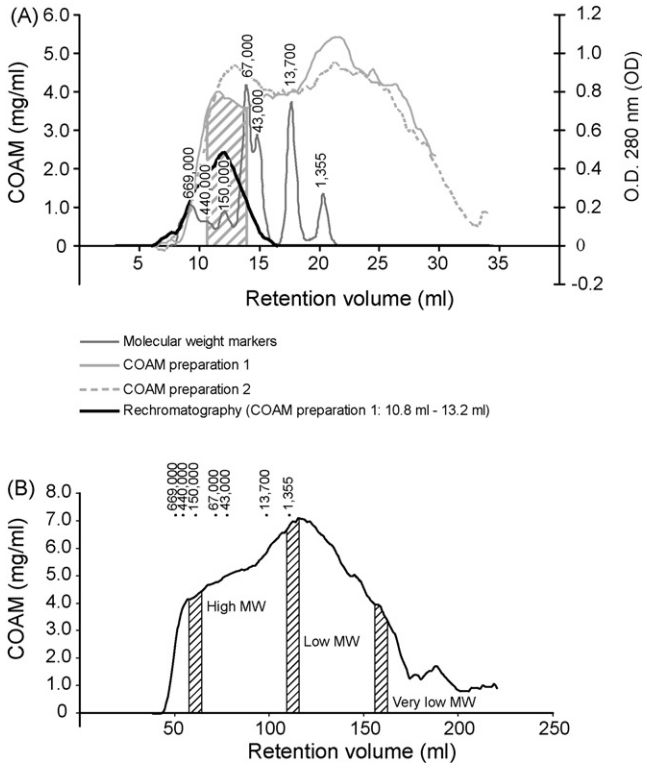

Fig. 2 – Gel filtration chromatography of COAM. (A) Analytical fractionation. Fifty milligrams of the COAM mixture was separated by gel filtration chromatography on a Superdex 200 10/300 GL column. After fractionation of COAM, pooled high molecular weight (MW) fractions were applied and eluted on the same gel matrix. This resulted in the expected similar elution position, which implies the chemical stability of the fractions. The hatched area indicates the pooled fractions. (B) For preparative fractionation of COAM, 700 mg of the mixture was separated on a Hiload 16/60 Superdex 200 column. A rechromatography of pooled fractions eluted at the same positions (shown as hatched areas). Both columns were first equilibrated and calibrated with a mixture of protein standards. The elution positions of these proteins are indicated in Da as size references, ranging from thyroglobulin (669 kDa), ferritin (440 kDa), IgG (150 kDa), bovine serum albumin (67 kDa), ovalbumin (43 kDa), cytochrome c (13 kDa) to vitamin B12 (1355 Da).

and the low stability of the polymer in the gas phase, the COAM molecules were fragmented in source during the electrospray ionisation. The resulting fragmentation pattern in the mass spectrum revealed the polymeric nature of the molecule, with alternating 'subunits' of 118 and 74 Da (Fig. 1B). These alternating subunits originate from the chlorite oxidation of the glucose units of amylose during the synthesis of COAM and correspond with its predicted structure. The complexity of the mass spectrum is also in part due to the presence of Na^+ adducts (addition of 22 Da) and partially dehydrated species (−18 Da), which are probably formed during the ionisation. One of the ions (574.8 Da) was isolated in the trap and further fragmented (Fig. 1C), showing that this ion consisted of 3 'subunits' of 118 Da alternated with 3 'subunits' of 74 Da. These results confirm the predicted structure of the COAM unit.

With further quality controls of the synthetic product it was established that COAM was endotoxin-free (less than 13.3 pg/mg) and devoid of protein contamination as determined by both Coomassie Blue and silver staining following gel electrophoresis. The COAM mixture is water-soluble and was fractionated by gel filtration chromatography as shown in Fig. 2. A standard protein preparation was used to calibrate the gel matrix and the COAM fractions were expressed in relation to these protein standards. The reproducible separations were collected in three different fractions according to molecular weight (MW), corresponding to high MW, low MW and very low MW COAM polymer fractions. Upon rechromatography, the selected high MW COAM preparation eluted at a similar retention volume as the pooled fraction. These observations showed that the fractions were chemically stable, that no interaction occurred between COAM and the column matrix and that the COAM polymers possessed a heterogenic MW.

3.2. *COAM is not an IFN inducer*

In previous studies, the mechanism of antiviral resistance of COAM was partly explained by the induction of IFN [9], as small amounts of the cytokine were detected in vivo. Other authors questioned this explanation [33], eventually suggesting that the IFN, induced in vivo, results from the virus challenge. Meanwhile, however, the mechanism of action of poly(I:C) is established to be by TLR-3-mediated IFN induction. Therefore, we investigated whether COAM could enhance the in vitro expression of IFN-α and -β and RLRs, in comparison with poly(I:C), by the sensitive measurement of mRNA levels. L929 cells were incubated with COAM or poly(I:C) and after the indicated time period, cell extracts were subjected to qRT-PCR. Our results, shown in Fig. 3, demonstrated that poly(I:C) significantly upregulated the expression of RIG-I (Fig. 3A) at 4, 8 and 16 h incubation. Likewise, the incubation of poly(I:C) induced a significant increase of MDA-5 mRNA at 4 and 8 h incubation time (Fig. 3B). The upregulation of both RIG-I and MDA-5 by poly(I:C) as early-expression genes significantly decreased in a time-dependent manner. For IFN-β, mRNA levels started to rise significantly at 16 h after induction with poly(I:C) and increased time-dependently (Fig. 3C). A significant upregulation of IFN-α4 mRNA was detected after 16 h of incubation with poly(I:C) (Fig. 3D). This observation is in line with a previous published report [34]. On the contrary, the mRNA expression levels of the RNA helicases and IFN-α and -β remained unaltered when cells were incubated with COAM (Fig. 3A-D). The mRNA analysis of IFN-α and -β was comparable to the amounts of secreted IFN protein measured by ELISA. No IFN-β protein secretion by L929 cells was detected after incubation with COAM (Fig. 4). Similar to the mRNA analysis, poly(I:C) significantly stimulated the secretion of IFN-β (Fig. 4). IFN-α protein levels remained below the detection limit of the assay for both the COAM and poly(I:C) incubations (data not shown). Although COAM and poly(I:C) share similar polyanionic features, they differed from each other in the potential to induce IFNs and RLRs. In contrast with poly(I:C), these results show that the antiviral effect of COAM can not be

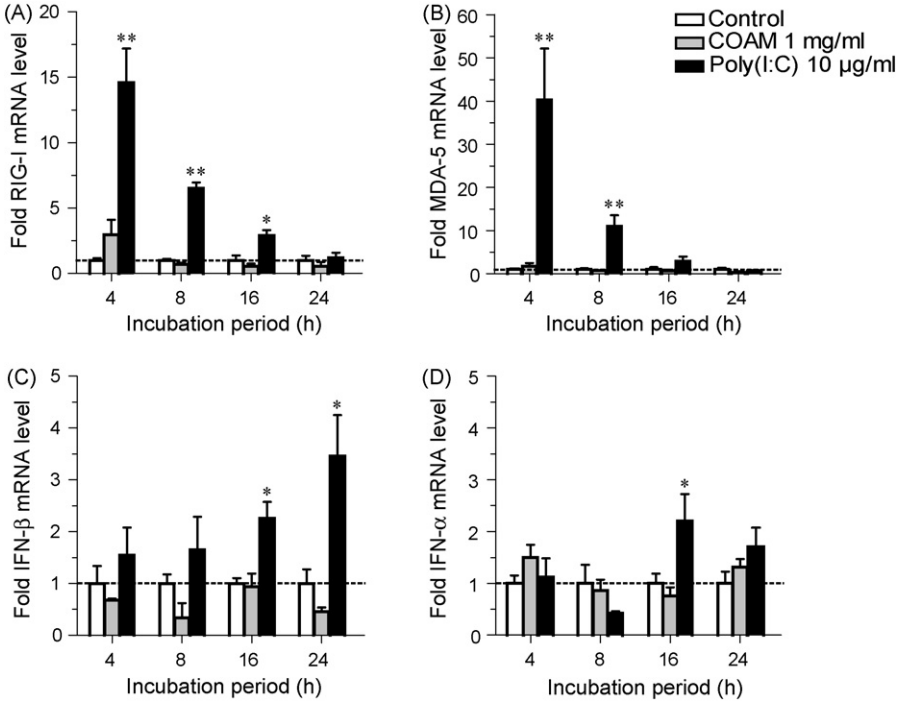

Fig. 3 – COAM does not act as an inducer of RIG-I-like receptors and IFNs. Monolayers of L929 cells were incubated with 1 mg/ml COAM or 10 μg/ml poly(I:C) for various time intervals. After the indicated incubation period, cells were disrupted and lysed and total cellular RNA was subjected to qRT-PCR. RIG-I (A), MDA-5 (B), IFN-β (C) and IFN-α4 (D) mRNA expression levels were measured and normalized against untreated controls. Dotted lines represent the threshold for determination of fold expression levels. Data represent mean values ± S.E.M. of three independent experiments. Compared with the cell controls, significant *p*-values of $p < 0.05$ (*) and $p < 0.005$ (**) were obtained.

addressed to a direct or indirect induction of an antiviral state through IFN upregulation by activation of RLR gene expression.

3.3. *The antiviral effect of COAM is dependent on polymer length*

To study further the mechanism of action of COAM, a set of in vitro experiments was conducted to evaluate if COAM might exert an inhibitory and dose-related antiviral effect on mengovirus infected mouse L929 cells. The potential in vitro activity of COAM against mengovirus was first investigated by evaluation of cell viability as an indirect parameter. L929 cells were treated or not with different doses of COAM and challenged with 10 $CCID_{50}$ mengovirus. When the induced cytopathogenic effect (CPE) in untreated cells reached 90–100%, the cell viability was measured by the formazan-based MTS assay. The calculated percentage of protected cells depended on the COAM concentration. At least 200 μg/ml COAM was required to obtain a protective effect (Fig. 5A) and the 50% inhibitory concentration (IC_{50}) was more than 500 μg/ml. The cytotoxicity was measured in parallel with the antiviral activity. COAM concentrations of up to 2 mg/ml did not induce any cytotoxic effect in L929 cells in a comparison of cell viability between treated cells and untreated controls. In a next step, differences in antiviral activity between COAM fractions of varying polymer length were compared. COAM fractions ranging from high to very low MW were compared with the mixture of COAM in the formazan-based MTS assay (Fig. 5B). Fractions with high MW displayed a significant better antiviral profile in comparison with the mixture, yielding a 30 to nearly 40% better protection for 250 and 500 μg/ml, respectively. The administration of COAM molecules of low MW did not significantly differ from the mixture and provided an effective protection at high concentrations, whereas very low MW COAM molecules did not contribute to the antiviral effect.

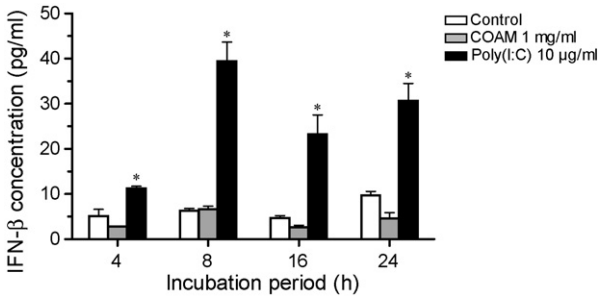

Fig. 4 – IFN-β protein secretion by L929 cells. Supernatants of L929 cells incubated with COAM or poly(I:C) were collected after the indicated incubation periods and the amount of secreted mouse IFN-β protein was determined by ELISA. Data represent mean values ± S.E.M. of at least three replicates. Significant *p*-values of $p < 0.05$ (*) were obtained for poly(I:C) incubations as compared to the cell controls.

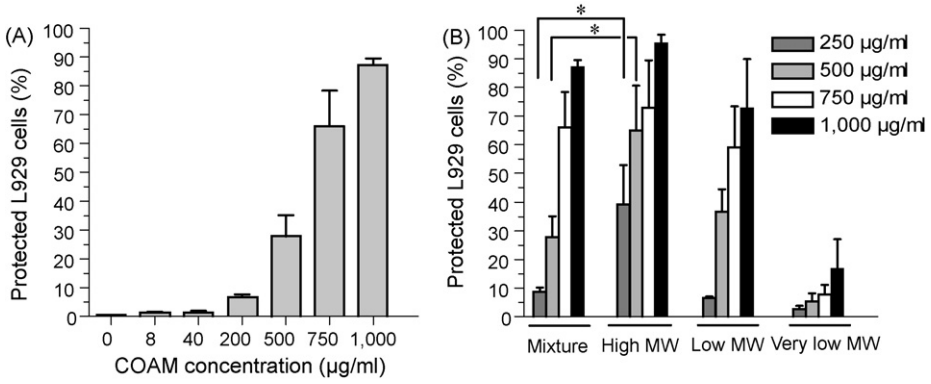

Fig. 5 – In vitro antiviral effect of COAM. L929 cells were challenged with mengovirus and treated with different concentrations of COAM in a 96-well format. (A) The viability of infected cells treated with different concentrations of COAM was colorimetrically analyzed with an MTS assay 2 days after virus inoculation with 10 $CCID_{50}$ mengovirus. The percentage of protected cells against virus infection was calculated. (B) COAM fractions of molecular weight (MW) ranging from high MW to very low MW were evaluated in comparison with the COAM mixture, based on the protection of cells two days after virus challenge with 10 $CCID_{50}$ mengovirus. In addition, uninfected cells without COAM addition and uninfected cells with COAM addition at 250, 500, 750, 1000 and 2000 μg/ml did not show any cytotoxicity. Significant *p*-values of $p < 0.05$ (*) were obtained between 250 and 500 μg/ml of the mixture compared with the high MW fraction. All data represent mean values ± S.E.M. of at least three independent experiments.

3.4. *Mengovirus quantitative RT-PCR and effect of COAM on mengovirus RNA replication*

In vitro transcribed mengovirus copy RNA (cRNA) molecules were used to generate a standard curve (Fig. 6A) which allowed the estimation of the absolute number of mengovirus genome copies in a sample. Duplicate tenfold dilutions of the cRNA standard corresponding to 2×10^1 to 2×10^8 mengovirus cRNA transcripts per reaction mixture were prepared and amplified in parallel with equal volumes of the samples. For each analysis, this resulted in a standard curve with a correlation coefficient of $\geq$0.99 which allowed to calculate the absolute number of virus RNA copies and to generate the linear regression curve. The detection limit of the mengovirus qRT-PCR assay was determined by amplifying, in triplicate, tenfold serial dilutions of the mengovirus standard ranging from 2 to 2×10^{12} cRNA transcripts. The results were analyzed in terms of the Ct value, which is the PCR cycle in which a target sequence is first detected. With the mengovirus qRT-PCR assay we were able to detect tenfold differences in concentration over a range from 2×10^1 to 2×10^8 RNA copies per reaction resulting in a dynamic range that covers 7 $\log_{10}$ units, with corresponding Ct values spanning from 38.22 ± 0.29 to 15.40 ± 0.06 (Fig. 6B). Alternatively to an indirect measurement of antiviral activity based on cell viability, the effect of COAM was investigated by absolute quantitation of mengovirus genome equivalents in supernatants of infected L929 cells. Mengovirus qRT-PCR results were analyzed in terms of the inhibition of virus replication as shown in Fig. 6C. COAM displayed a dose-dependent reduction in virus replication with inhibition percentages of more than 50% for COAM concentrations higher than 2 μg/ml. Concentrations of 500 μg/ml COAM and higher yielded nearly 100% inhibition of virus replication. The lowest concentration tested, 0.08 μg/ml, still yielded an average inhibition of virus replication of 13.6%. Thus, in this experimental system, viral progeny determination through qRT-PCR was a more sensitive method for the detection of an antiviral effect than the cell viability assay. Furthermore, no direct inactivating effect, based on cell viability, of COAM against mengovirus was observed when COAM was incubated with the virus prior to infection (data not shown).

3.5. *COAM inhibits mengovirus entry*

Time-of-addition experiments were performed to investigate the effect of COAM on the virus replicative cycle, by treatment of L929 cells with 1 mg/ml COAM at different time points after infection. An administration scheme is given in Fig. 7A. When administered simultaneously with the virus at the start of infection and removed again 1 h p.i., COAM was thus allowed to interact with the host cells only at a very early replication stage of the virus. When administered at later time points up to 7 h p.i., the post-adsorption replication stages, early or late, can be ruled out as contributing to the antiviral effect. Twelve hours p.i. cell culture supernatants were collected and subjected to mengovirus qRT-PCR and absolute virus quantities were converted to the percentage virus replication. The results showed that COAM almost completely inhibited virus replication when added at 0–1 h, during virus adsorption, or at 0–12 h, during and after virus adsorption (Fig. 7B). When COAM was added at later time points, starting at 1 h p.i. and thus after adsorption, virus replication increased, indicating that COAM affects an early stage of mengovirus infection. The inhibitory effect of COAM on early steps of mengovirus replication was also investigated by assessing the amount of bound virus particles when different concentrations of COAM were present during 1 h viral attachment at 4 °C. As illustrated in Fig. 7C, mengovirus attachment was inhibited by 74.3% at a high concentration of COAM (1000 μg/ml). Thus, COAM was

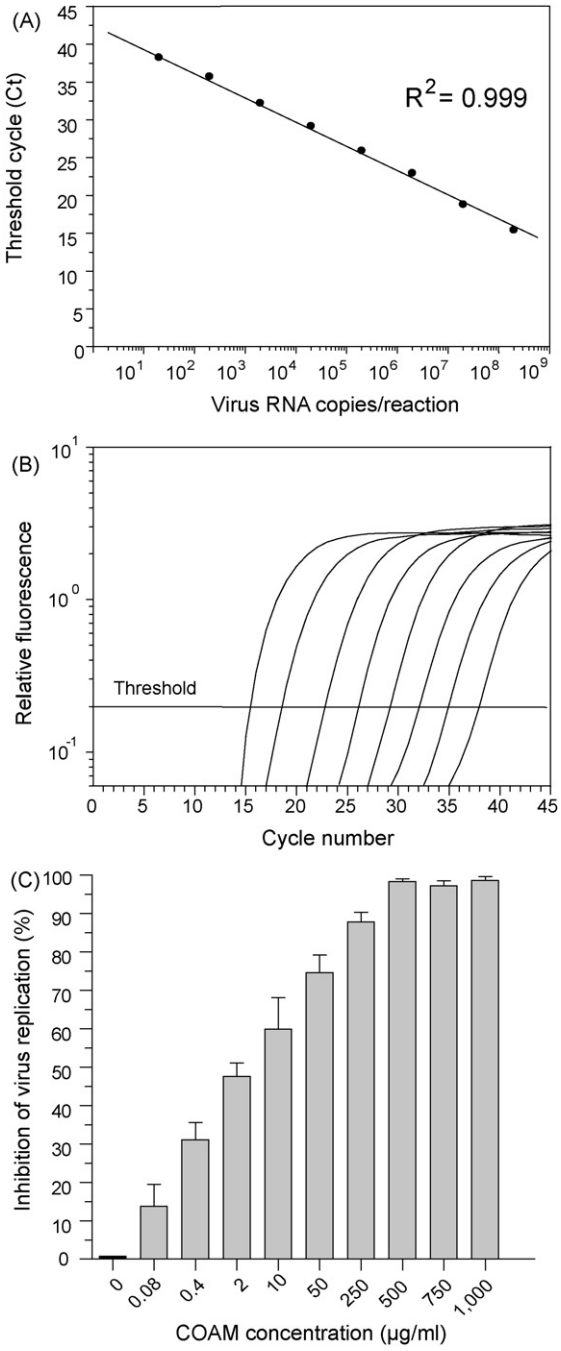

Fig. 6 – Effect of COAM on mengovirus progeny detection with qRT-PCR. (A) Tenfold serial dilutions ranging from 2×10^1 to 2×10^8 in vitro transcribed mengovirus cRNA molecules allowed to construct a standard curve with a slope of −3.74 and a correlation coefficient of 0.999. Cycle threshold (Ct) values are plotted against the input amounts of mengovirus cRNA. The Ct value to detect a single target molecule, the Y-intercept, was 42.40. (B) qRT-PCR reactions of tenfold serial dilutions of the mengovirus cRNA standard were analyzed to determine the detection limit of the assay. The amplification graph was generated by plotting the normalized fluorescence against the qRT-PCR cycle number. The dynamic range of the qRT-PCR assay covers 7 $\log_{10}$ units. (C) Cells were treated with different concentrations of COAM and subsequently infected with 10 $CCID_{50}$ mengovirus. One day post-infection, the culture supernatants were collected, viral RNA was extracted and the reduction of virus replication was measured with mengovirus qRT-PCR. Antiviral activity was estimated in terms of the percentage of inhibition of virus replication. All data represent mean values ± S.E.M. of at least six replicates.

effective at inhibiting the infectivity of mengovirus particles that had been prebound at 4 °C. We also checked whether COAM might shield the virus directly, thus preventing attachment or entry. However, virus preparations containing 10 $CCID_{50}$ pretreated with COAM concentrations up to 1000 μg/ml and thereafter diluted 100 times retained full infectivity comparable to that of 0.1 $CCID_{50}$. In conclusion, the antiviral resistance of COAM can be attributed to an interaction with early steps in the virus replication cycle, most likely during virus attachment and a high dose of 1000 μg/ml COAM is necessary to obtain a direct antiviral effect in vitro.

4. Discussion

Early studies on polyacetal carboxylic acids as a group of antiviral polyanions indicated that COAM is a promising antiviral agent against a broad spectrum of viruses [6,7,9]. Unfortunately, comprehensive investigations on the mode of action remained insufficiently established. In this study we first performed a refined biochemical analysis and extensive quality control of COAM preparations. COAM was thus subjected to ion-trap mass spectrometry analysis, which showed a repetitive pattern of peaks. In this way, the structural unit of the polymer was corroborated. In addition, the COAM preparation was characterized to be devoid of protein and endotoxin contamination. Furthermore, with the use of gel filtration chromatography, COAM fractions with different polymer sizes were isolated. Three major MW fractions were separated and compared in vitro. The data indicated that COAM fractions of high MW (long polymer chains) showed an enhanced antiviral effect when compared with low MW COAM. This finding is in line with the previous observation that other antiviral polyanions like dextran sulphate, show a marked enhancement of antiviral activity when the MW increased [11]. For polyanions in general, large molecules (≥5 kDa) with sufficient negative charges are indispensable in order to exert efficient in vitro antiviral activity [35]. Indeed, our results showed that COAM fractions of very low MW displayed little antiviral activity on cell culture, whereas fractions of higher MW were more efficient. Comparing the antiviral effect of COAM in vitro and in vivo [9], the dose of COAM required to obtain an in vivo effect is 10–100 times lower than the concentration needed for the same in vitro effect, if one considers an equal distribution in vivo. Either the effect of COAM in vivo is aided by bystander immunological mechanisms, or the local concentrations of the product might be higher than those based on an equal body distribution or a combination.

Former attempts in exploring the mechanism of antiviral resistance of COAM were primarily focused on the modification of the host antiviral response, in particular through the

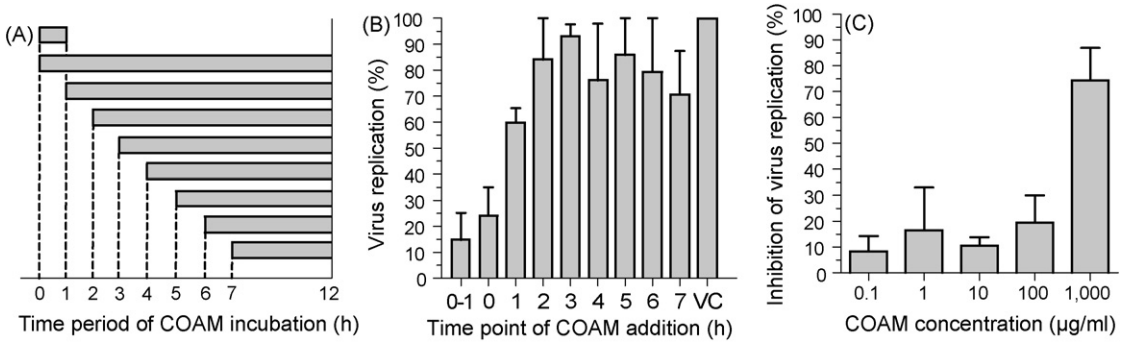

Fig. 7 – COAM interacts with early steps of virus replication. (A) Time-of-addition scheme. COAM was administered to confluent L929 monolayers during different time periods of a mengovirus replication cycle. Grey horizontal bars indicate the time point from which COAM was added and the duration of incubation on mengovirus infected cells. (B) Twelve hours after virus infection, cell culture supernatants were collected and the extracellular mengovirus replication was evaluated by viral RNA quantitation with qRT-PCR. Data represent mean values ± S.E.M. of three independent experiments. VC = virus control. (C) The effect of COAM on mengovirus attachment was studied by incubating L929 monolayers with 100 $CCID_{50}$ mengovirus at 4 °C for 1 h in the presence of various concentrations of the test compound. Unattached virus particles and compound were removed by washing the cells with PBS. After a further incubation of 8 h, the amount of bound virus particles was measured in terms of viral RNA copies using mengovirus qRT-PCR. Data represent mean values ± S.E.M. of six different cell cultures.

IFN pathway. By systemic administration of a high dose of COAM small amounts of IFN were detectable in the circulation after viral challenge [9]. Some studies even reported that COAM acted as an adjuvant upon treatment with poly(I:C), hereby increasing the serum IFN titer 6- to 100-fold [33,36]. However, such a combined treatment did not increase the protection against infection and COAM alone did not induce measurable levels of IFN [36]. Poly(I:C), an established IFN-inducing agent, is structurally similar to COAM, based upon their polyanionic natures. The present study, however, provides evidence that COAM does not share the IFN enhancing capacity of poly(I:C). Hence, the antiviral effect of COAM must be attributed to other mechanisms, as upregulation of IFN-α and -β and of RNA helicases RIG-I and MDA-5 was absent in vitro.

In general, antiviral polyanions appear to interact with the fusion of the virus with its target cell membrane. Some anionic polymers are believed to interact specifically with the virus rather than with the cell membrane, as shown for heparin and dextran sulphate, which exert virucidal activity against EMCV and Theiler's encephalomyelitis virus [37,38]. From our results, however, it was deduced that COAM did not inactivate the virus particle in its extracellular state, thus supporting the view that COAM did not combine with the virus particle. The time-of-addition and attachment assays indicated that COAM is likely to interfere with very early steps of the virus replicative cycle, at a stage when infection is not yet fully established. Taken together, these data point to the attachment of the virus to the cell membrane as the target of antiviral action. Most likely COAM inhibits the attachment through formation of a shielding matrix against the virus on cell membrane receptors.

In conclusion, this study provides evidence that COAM displays distinctive antiviral actions, compared to other polyanions, such as poly(I:C). Our results reinforce the idea that COAM – unlike poly(I:C) – is not an IFN enhancer, but instead exerts its antiviral effect by prohibiting virus attachment.

Acknowledgments

The authors thank all the colleagues of the Laboratory of Immunobiology for helpful discussions and advice. This study was supported by the Centre of Excellence (EF/05/015), the 'Geconcerteerde OnderzoeksActies' (GOA), the Belgian Charcot Foundation and the Fund for Scientific Research-Flanders (FWO-Vlaanderen). PVDS is a postdoctoral fellow of the FWO-Vlaanderen.

REFERENCES

[1] Karpas A, Fleet GW, Dwek RA, Petursson S, Namgoong SK, Ramsden NG, et al. Aminosugar derivatives as potential anti-human immunodeficiency virus agents. Proc Natl Acad Sci USA 1988;85:9229–33.
[2] Block TM, Lu X, Platt FM, Foster GR, Gerlich WH, Blumberg BS, et al. Secretion of human hepatitis B virus is inhibited by the imino sugar N-butyldeoxynojirimycin. Proc Natl Acad Sci USA 1994;91:2235–9.
[3] Branza-Nichita N, Durantel D, Carrouee-Durantel S, Dwek RA, Zitzmann N. Antiviral effect of N-butyldeoxynojirimycin against bovine viral diarrhea virus correlates with misfolding of E2 envelope proteins and impairment of their association into E1–E2 heterodimers. J Virol 2001;75:3527–36.
[4] Zitzmann N, Mehta AS, Carrouee S, Butters TD, Platt FM, McCauley J, et al. Imino sugars inhibit the formation and secretion of bovine viral diarrhea virus, a pestivirus model of hepatitis C virus: implications for the development of broad spectrum anti-hepatitis virus agents. Proc Natl Acad Sci USA 1999;96:11878–82.

[5] Wu SF, Lee CJ, Liao CL, Dwek RA, Zitzmann N, Lin YL. Antiviral effects of an iminosugar derivative on flavivirus infections. J Virol 2002;76:3596–604.
[6] Claes P, Billiau A, De Clercq E, Desmyter J, Schonne E, Vanderhaeghe H, et al. Polyacetal carboxylic acids: a new group of antiviral polyanions. J Virol 1970;5:313–20.
[7] Billiau A, Muyembe JJ, De Somer P. Effect of chlorite-oxidized oxyamylose on influenza virus infection in mice. Appl Microbiol 1971;21:580–4.
[8] Leunen J, Desmyter J, De Somer P. Effects of oxyamylose and polyacrylic acid on foot-and-mouth disease and hog cholera virus infections. Appl Microbiol 1971;21:203–8.
[9] Billiau A, Desmyter J, De Somer P. Antiviral activity of chlorite-oxidized oxyamylose, a polyacetal carboxylic acid. J Virol 1970;5:321–8.
[10] De Clercq E, Luczak M. Intranasal challenge of mice with herpes simplex virus: an experimental model for evaluation of the efficacy of antiviral drugs. J Infect Dis 1976;133(Suppl):A226–36.
[11] Baba M, Snoeck R, Pauwels R, De Clercq E. Sulfated polysaccharides are potent and selective inhibitors of various enveloped viruses, including herpes simplex virus, cytomegalovirus, vesicular stomatitis virus, and human immunodeficiency virus. Antimicrob Agents Chemother 1988;32:1742–5.
[12] Hosoya M, Balzarini J, Shigeta S, De Clercq E. Differential inhibitory effects of sulfated polysaccharides and polymers on the replication of various myxoviruses and retroviruses, depending on the composition of the target amino acid sequences of the viral envelope glycoproteins. Antimicrob Agents Chemother 1991;35:2515–20.
[13] Lederman S, Gulick R, Chess L. Dextran sulfate and heparin interact with CD4 molecules to inhibit the binding of coat protein (gp120) of HIV. J Immunol 1989;143:1149–54.
[14] Weber F, Wagner V, Rasmussen SB, Hartmann R, Paludan SR. Double-stranded RNA is produced by positive-strand RNA viruses and DNA viruses but not in detectable amounts by negative-strand RNA viruses. J Virol 2006;80:5059–64.
[15] Alexopoulou L, Holt AC, Medzhitov R, Flavell RA. Recognition of double-stranded RNA and activation of NF-kappaB by toll-like receptor 3. Nature 2001;413:732–8.
[16] Yamamoto M, Sato S, Hemmi H, Hoshino K, Kaisho T, Sanjo H, et al. Role of adaptor TRIF in the MyD88-independent toll-like receptor signaling pathway. Science 2003;301:640–3.
[17] Guillot L, Le Goffic R, Bloch S, Escriou N, Akira S, Chignard M, et al. Involvement of toll-like receptor 3 in the immune response of lung epithelial cells to double-stranded RNA and influenza A virus. J Biol Chem 2005;280:5571–80.
[18] Rudd BD, Burstein E, Duckett CS, Li X, Lukacs NW. Differential role for TLR3 in respiratory syncytial virus-induced chemokine expression. J Virol 2005;79:3350–7.
[19] Ashkar AA, Yao XD, Gill N, Sajic D, Patrick AJ, Rosenthal KL. Toll-like receptor (TLR)-3, but not TLR4, agonist protects against genital herpes infection in the absence of inflammation seen with CpG DNA. J Infect Dis 2004;190:1841–9.
[20] Tabeta K, Georgel P, Janssen E, Du X, Hoebe K, Crozat K, et al. Toll-like receptors 9 and 3 as essential components of innate immune defense against mouse cytomegalovirus infection. Proc Natl Acad Sci USA 2004;101:3516–21.
[21] Gitlin L, Barchet W, Gilfillan S, Cella M, Beutler B, Flavell RA, et al. Essential role of mda-5 in type I IFN responses to polyriboinosinic:polyribocytidylic acid and encephalomyocarditis picornavirus. Proc Natl Acad Sci USA 2006;103:8459–64.
[22] Kang DC, Gopalkrishnan RV, Wu Q, Jankowsky E, Pyle AM, Fisher PB. mda-5: an interferon-inducible putative RNA helicase with double-stranded RNA-dependent ATPase activity and melanoma growth-suppressive properties. Proc Natl Acad Sci USA 2002;99:637–42.
[23] Yoneyama M, Kikuchi M, Natsukawa T, Shinobu N, Imaizumi T, Miyagishi M, et al. The RNA helicase RIG-I has an essential function in double-stranded RNA-induced innate antiviral responses. Nat Immunol 2004;5:730–7.
[24] Yoneyama M, Kikuchi M, Matsumoto K, Imaizumi T, Miyagishi M, Taira K, et al. Shared and unique functions of the DExD/H-box helicases RIG-I, MDA5, and LGP2 in antiviral innate immunity. J Immunol 2005;175:2851–8.
[25] Kato H, Sato S, Yoneyama M, Yamamoto M, Uematsu S, Matsui K, et al. Cell type-specific involvement of RIG-I in antiviral response. Immunity 2005;23:19–28.
[26] Kato H, Takeuchi O, Sato S, Yoneyama M, Yamamoto M, Matsui K, et al. Differential roles of MDA5 and RIG-I helicases in the recognition of RNA viruses. Nature 2006;441:101–5.
[27] Borden EC, Sen GC, Uze G, Silverman RH, Ransohoff RM, Foster GR, et al. Interferons at age 50: past, current and future impact on biomedicine. Nat Rev Drug Discov 2007;6:975–90.
[28] Takaoka A, Yanai H. Interferon signalling network in innate defence. Cell Microbiol 2006;8:907–22.
[29] Maes P, Li S, Verbeeck J, Keyaerts E, Clement J, Van Ranst M. Evaluation of the efficacy of disinfectants against Puumala hantavirus by real-time RT-PCR. J Virol Methods 2007;141:111–5.
[30] Fronhoffs S, Totzke G, Stier S, Wernert N, Rothe M, Bruning T, et al. A method for the rapid construction of cRNA standard curves in quantitative real-time reverse transcription polymerase chain reaction. Mol Cell Probes 2002;16:99–110.
[31] Livak KJ, Schmittgen TD. Analysis of relative gene expression data using real-time quantitative PCR and the 2(-Delta Delta C(T)) method. Methods 2001;25:402–8.
[32] Pauwels R, Balzarini J, Baba M, Snoeck R, Schols D, Herdewijn P, et al. Rapid and automated tetrazolium-based colorimetric assay for the detection of anti-HIV compounds. J Virol Methods 1988;20:309–21.
[33] Levy HB, Duenwald J, Buckler CE. Chlorite-oxidized amylose as an adjuvant for interferon production. Infect Immun 1973;7:457–60.
[34] van Pesch V, Lanaya H, Renauld JC, Michiels T. Characterization of the murine alpha interferon gene family. J Virol 2004;78:8219–28.
[35] Luscher-Mattli M. Polyanions—a lost chance in the fight against HIV and other virus diseases? Antivir Chem Chemother 2000;11:249–59.
[36] Harmon MW, Janis B, Levy HB. Post-exposure prophylaxis of murine rabies with polyinosinic–polycytidylic acid and chlorite-oxidized amylose. Antimicrob Agents Chemother 1974;6:507–11.
[37] Liebhaber H, Takemoto KK. The basis for the size differences in plaques produced by variants of encephalomyocarditis (EMC) virus. Virology 1963;20:559–66.
[38] Mandel B. Inhibition of Theiler's encephalomyelitis virus (GDVII strain) of mice by an intestinal mucopolysaccharide. III. Studies on factors that influence the virus-inhibitor reaction. Virology 1957;3:444–63.